Field-Effect Transistors Based on Thiophene Hexamer Analogues with Diminished Electron Donor Strength

Wenjie Li,* Howard E. Katz,* Andrew J. Lovinger, and Joyce G. Laquindanum

Bell Laboratories, Lucent Technologies, 600 Mountain Avenue, Murray Hill, New Jersey 07974

Received September 24, 1998. Revised Manuscript Received November 19, 1998

Several new p-type semiconducting materials with lower electron-donating ability than the parent sexithiophene were synthesized and their thermal, morphological, and FET properties were investigated. The incorporation of thiazole rings into oligothiophenes was designed to lower the highest occupied molecular orbital (HOMO) level of the molecules and hence make them less susceptible to p-doping. FET devices based on a dihexylated six-ring compound with thiazoles as the central rings indeed showed enhanced stability to p-doping over those of typical sexithiophenes. Relatively high on/off current ratios (greater than 10^4 for gate voltages of −100 and 0 V) were routinely obtained from devices operating in air, eliminating the need for strict exclusion of oxygen. The threshold voltage of devices made from this compound showed no signs of shifting toward more positive gate voltages after more than one month's exposure to the air. The thiazole-containing oligomers generally had lower field-effect mobilities than the corresponding oligothiophenes, possibly due to larger charge injection barrier and less favorable morphologies of the evaporated films. The electrical characteristics of the previously uninvestigated α,ω-dihexyl quinquethiophene (DHα5T) are also reported in this paper. Single-crystal morphologies were observed in evaporated films of DHα5T. Films evaporated at an optimal deposition temperature (T_D = 155 °C) gave mobilities as high as 0.1 cm^2/Vs. As in the cases of pentacene and DHα4T, we believe that the greatly enhanced mobility is probably correlated with the single-crystal morphology. DHα5T molecules also have an orientation different from the essentially perpendicular one of other oligothiophenes; they were found to be tilted at ∼30° to the substrate.

Introduction

Organic and polymeric semiconductors are currently attracting increasing attention as potential active components in many electronic or optical devices including field-effect transistors (FETs).[1] In a FET device, the semiconductor layer supports a channel of holes (p-type) or electrons (n-type) between the source and drain electrodes. The density of charge carriers in the channel is modulated by the voltage applied through the gate electrode. The most important criteria for a FET semiconductor are high charge carrier mobility, high current modulation (on/off current ratio), stability, and processability. A variety of organic structures have been demonstrated to be active p-channel materials, including a group of linear, conjugated molecules such as oligothiophenes,[2] carbon−sulfur fused rings,[3−5] pentacene,[6] polythiophenes,[7] polythienylenevinylenes,[8] polypyrroles,[9] and phthalocyanines.[10] High field-effect mobilities of above 0.01 cm^2/Vs and high on/off current ratios of greater than 10^6 have been achieved in some of the systems under carefully controlled conditions such as strict exclusion of oxygen and material purification or in situations where a substantial part of the switching occurs in the depletion mode (positive gate voltages for hole-transporting materials).[2−6]

Furthermore, most of the materials have very limited solubility in organic solvents, which makes liquid phase processing impossible in these systems. To truly realize the advantages of organic materials in FET applications, liquid-phase processable materials are important in order to fabricate devices using low-cost techniques such as casting, spin-coating, or printing. Recently, FET devices based on regioregular poly(3-alkylthiophene)s

(1) For recent reviews on organic FETs, see: (a) Katz, H. E. *J. Mater. Chem.* **1997**, *7*, 369. (b) Horowitz, G. *Adv. Mater.* **1998**, *10*, 365.

(2) Garnier, F.; Horowitz, G.; Peng, X. Z.; Fichou, D. *Synth. Met.* **1991**, *45*, 163. (b) Servet, B.; Horowitz, G.; Ries, S.; Lagorsse, O.; Alnot, P.; Yassar, A.; Deloffre, F.; Srivastava, P.; Hajlaoui, R.; Lang, P.; Garnier, F. *Chem. Mater.* **1994**, *6*, 1809. (c) Dodabalapur, A.; Torsi, L.; Katz, H. E. *Science* **1995**, *268*, 270.

(3) Laquindanum, J. G.; Katz, H. E.; Lovinger, A. J.; Dodabalapur, A. *Adv. Mater.* **1997**, *9*, 36.

(4) Li, X.-C.; Sirringhaus, H.; Garnier, F.; Holmes, A. B.; Moratti, S. C.; Feeder, N.; Clegg, W.; Teat, S. J.; Friend, R. H. *J. Am. Chem. Soc.* **1998**, *120*, 2206.

(5) Laquindanum, J. G.; Katz, H. E.; Lovinger, A. J. *J. Am. Chem. Soc.* **1998**, *120*, 664.

(6) Laquindanum, J. G.; Katz, H. E.; Lovinger, A. J.; Dodabalapur, A. *Chem. Mater.* **1996**, *8*, 2542. (b) Lin, Y. Y.; Gundlach, D. J.; Jackson, T. N. *54th Annual Device Research Conference Digest*; IEEE: Santa Barbara, CA, 1996, p 75. Also: *Science* **1996**, *273*, 879. (c) Dimitrakopoulos, C. D.; Brown, A. R.; Pomp, A. J. *J. Appl. Phys.* **1996**, *80*, 2501.

(7) Tsumura, A,; Koezuka, H.; Ando, T. *Appl. Phys. Lett.* **1986**, *49*, 1210. (b) Taylor, D. M.; Gomes, H. L.; Underhill, A. E.; Clemenson, P. I. *J. Phys. D: Appl. Phys.* **1991**, *24*, 2032. (c) Kou, C.-T.; Liou, T.-R. *Synth. Met.* **1996**, *82*, 167.

(8) Fuchigami, H.; Tsumura, A.; Koezuka, H. *Appl. Phys. Lett.* **1993**, *63*, 1372.

(9) Jarrett, C. P.; Friend, R. H.; Brown, A. R.; de Leeuw, D. M. *J. Appl. Phys.* **1995**, *77*, 6289.

(10) Bao, Z.; Lovinger, A. J.; Dodabalapur, A. *Appl. Phys. Lett.* **1996**, *69*, 3066. (b) Bao, Z.; Lovinger, A. J.; Dodabalapur, A. *Adv. Mater.* **1997**, *9*, 42.

10.1021/cm980672c CCC: $18.00
Published on Web 01/20/1999

have been shown to have mobilities in the range of 0.01−0.1 cm^2/Vs.[11] The high mobility is attributed to better ordering of the polymer film induced by the regioregular head-to-tail coupling of the alkyl side chains. Because of the good solubility and processability of these polymers, large area devices could be obtained by simple casting, spin-coating, or screen printing techniques.[11] Although high on/off ratios (10^4−10^6) were achieved by optimizing device fabrication (reducing unintentional doping and processing the device under inert atmosphere such as vacuum or dry N_2), off currents of poly(3-alkylthiophene) FET devices are usually high due to impurities and structural defects within the polymers.

Our research efforts in FETs have been focused on identifying organic materials with high performance, good solubility, and potential liquid phase processability, as well as long-term stability. We have previously reported an investigation of the synthesis and semiconducting properties of thiophene oligomers with solubilizing end-substituents, especially α,ω-dihexylsexithiophene (DHα6T) and α,ω-dihexylquarterthiophene (DHα4T),[12−14] the use of which was first suggested by Garnier and co-workers.[15,16] Unlike the thiophene polymers, impurities in these oligothiophenes can be relatively easily removed by sublimation under reduced pressure. The monodisperse conjugation length of these molecules allows them to organize into almost defect-free layered structures. Thin film FETs with high mobility can be routinely obtained by evaporation. FET devices were also fabricated by casting dilute solutions of these compounds. The highest mobilities (ca. 0.03 cm^2/Vs) were achieved with DHα6T, approaching the values of the evaporated films of the same compound. This casting process may be useful in devising all-liquid-phase fabrication protocols for organic-based circuits. Nevertheless, the DHα6T solution is still susceptible to doping, so that a better on/off ratio (>10^3) can only be achieved by careful purification of the compound and strict control of the measurement conditions.

It has been known that the introduction of an imino nitrogen into a thiophene ring could increase its electron-withdrawing ability and hence make it less susceptible to p-doping (oxidation). Several thiazole- and bithiazole-containing polymers were recently synthesized and their electronic and optical properties were studied.[17−19] The redox potentials of the thiazole polymers generally appear at more positive values than those observed with thiophene polymers, revealing that the oxidation is more difficult for the thiazole polymers. X-ray diffraction analysis of regioregular poly(alkylbithiazoles) supports a face-to-face π-stacking of the polymer chains in the solid state, similar to what has been observed in regioregular poly(3-alkylthiophenes). These polymers have been employed in the construction of light-emitting diodes (LEDs).[18c,19d] However, to the best of our knowledge, no reports on thiazole-related compounds in FET applications have been made so far.

In this paper, we report on FETs made with several novel thiophene−thiazole co-oligomers, as well as with the previously uninvestigated dihexylquinquethiophene (DHα5T). The latter compound should be less easily doped than DHa6T, simply by virtue of its shorter conjugated core, which should provide lesser stabilization of its radical cation. Introduction of the thiazole rings should lower the orbital energies of the oligomers and therefore make them harder to dope. In addition, although the thiazole molecules have essentially the same geometry as thiophenes, the larger polarity of thiazoles could also influence the crystal growth of the oligomers. All of these compounds were synthesized using the Stille coupling reaction according to Scheme 1. In addition to the usual thermal and analytical characterization, the morphology and crystallinity of these compounds as evaporated thin films was also investigated. The morphology of one condensed ring compound, 5,6,11,12-tetraazanaphthacene (TAN), is reported as well. Mobilities and on/off ratios of FET devices made of the thiophene−thiazole oligomers were obtained and compared to those of the corresponding oligothiophenes. The liquid-phase fabrication of FET devices based on these compounds will be separately reported.

Experimental Section

All starting materials were purchased from Aldrich and used as received unless otherwise specified. Tetrahydrofuran (THF) was distilled from sodium benzophenone ketyl. 2,2′-Bithiazole (**1**),[20] 5,5′-bis(trimethylstannyl)-2,2′-bithiazole (**4**),[18] 5,5′-bis(2-thienyl)-2,2′-bithiazole (**T2Z2**),[18] 5-hexyl-5′-tributylstannyl-2,2′-bithiophene (**5**),[13] and 5,5′-dibromo-4,4′-dihexyl-2,2′-bithiazole (**6**)[19a] were synthesized according to the literature procedure. NMR spectra were collected on a Bruker 360 MHz spectrometer and referenced to tetramethylsilane. Thermal analyses were performed using a Perkin-Elmer DSC7 (differential scanning calorimetry) analyzer. Elemental analyses were done by Robertson Microlit Laboratories. Molecular modeling was performed using the Spartan version of the AM1 semiempirical method and Cerius software from Molecular Simulations, Inc.

Both "bottom" and "top" contact configurations were used to make the FET devices, as illustrated in Figure 1. The n-doped silicon substrate functions as the gate. A 3000 Å silicon dioxide dielectric layer with a capacitance per unit area of 1.1×10^{-8} F/cm^2 was thermally grown on the gate substrate.

(11) Bao, Z.; Dodabalapur, A.; Lovinger, A. J. *Appl. Phys. Lett.* **1996**, *69*, 4108. (b) Bao, Z.; Feng, Y.; Dodabalapur, A.; Raju, V. R.; Lovinger, A. J. *Chem. Mater.* **1997**, *9*, 1299. (c) Sirringhaus, H.; Tessler, N.; Friend, R. H. *Science* **1998**, *280*, 1741.

(12) Katz, H. E.; Dodabalapur, A.; Torsi, L.; Elder, D. *Chem. Mater.* **1995**, *7*, 2238.

(13) Katz, H. E.; Laquindanum, J. G.; Lovinger, A. J. *Chem. Mater.* **1998**, *10*, 633.

(14) Katz, H. E.; Lovinger, A. J.; Laquindanum, J. G. *Chem. Mater.* **1998**, *10*, 457.

(15) Garnier, F.; Yassar, A.; Hajlaoui, R.; Horowitz, G.; Deloffre, F.; Servet, B.; Ries, S.; Alnot, P. *J. Am. Chem. Soc.* **1993**, *115*, 8716.

(16) Garnier, F. presented at the Materials Research Society spring meeting, 1997, San Francisco, CA.

(17) Wolf, M. O.; Wrighton, M. S. *Chem. Mater.* **1994**, *6*, 1526.

(18) Maruyama, T.; Suganuma, H.; Yamamoto, T. *Synth. Met.* **1995**, *74*, 183. (b) Yamamoto, T.; Suganuma, H.; Maruyama, T.; Kubota, K. *J. Chem. Soc., Chem. Commun.* **1995**, 1613. (c) Yamamoto, T.; Suganuma, H.; Maruyama, T.; Inoue, T.; Muramatsu, Y.; Arai, M.; Komarudin, D.; Ooba, N.; Tomaru, S.; Sasaki, S.; Kubota, K. *Chem. Mater.* **1997**, *9*, 1217. (d) Yamamoto, T.; Komarudin, D.; Arai, M.; Lee, B.-L.; Suganuma, H.; Asakawa, N.; Inoue, Y.; Kubota, K.; Sasaki, S.; Fukuda, T.; Matsuda, H. *J. Am. Chem. Soc.* **1998**, *120*, 2047.

(19) Nanos, J. I.; Kampf, J. W.; Curtis, M. D. *Chem. Mater.* **1995**, *7*, 2232. (b) Ronda, L. G.; Martin, D. C. *Macromolecules* **1997**, *30*, 1524. (c) Curtis, M. D.; Cheng, H.; Johnson, J. A.; Nanos, J. I. *Chem. Mater.* **1998**, *10*, 13. (d) Politis, J. K.; Curtis, M. D.; Gonzalez, L.; Martin, D. C.; He, Y.; Kanicki, J. *Chem Mater.* **1998**, *10*, 1713.

(20) Dondoni, A.; Fogagnolo, M.; Medici, A.; Negrini, E. *Synthesis* **1987**, 185.

Scheme 1. Synthesis of the Thiazole-Containing Compounds and DHα5T

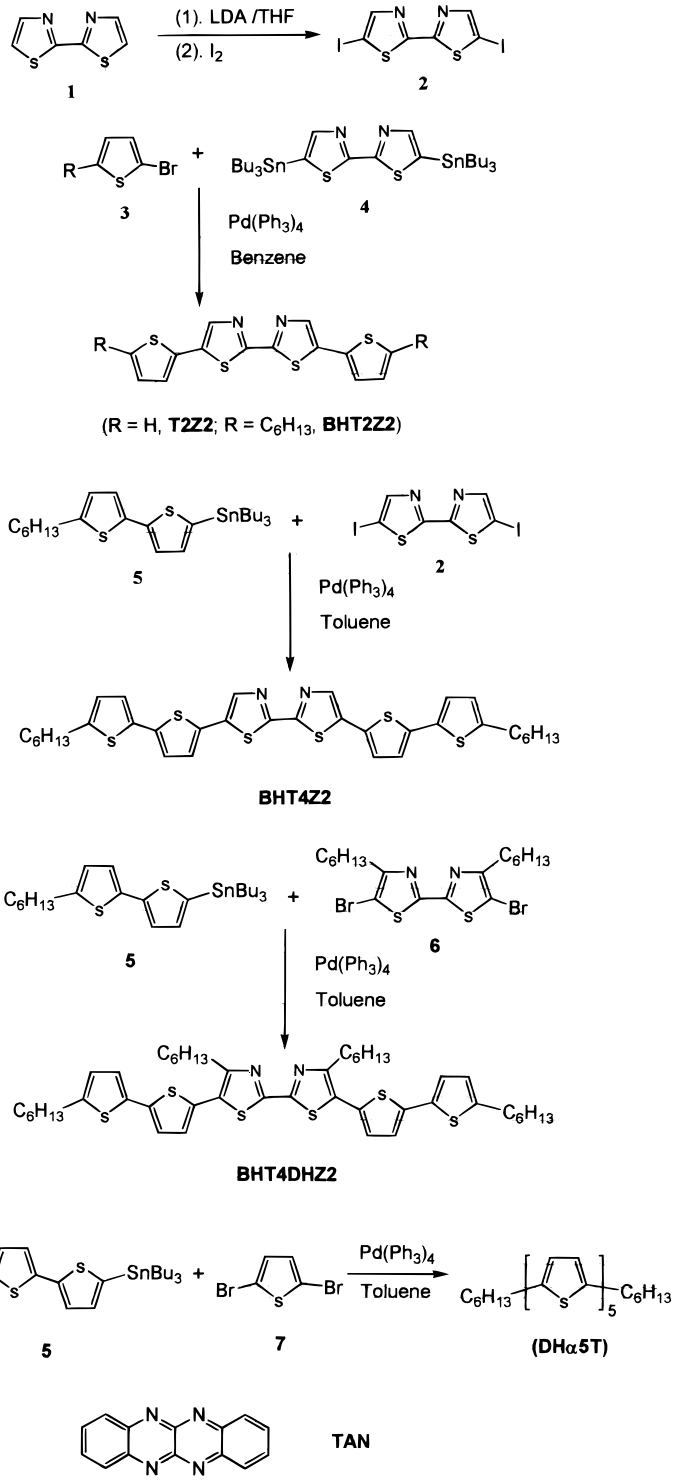

For the "bottom contact" geometry, gold electrodes forming channels of 250 μm width (W) and 1.5−25 μm length (L) were photolithographically defined. The semiconductor layer was then deposited over the entire electrode/dielectric surface. For the alternate "top contact" geometry, gold electrodes were defined after semiconductor deposition by using shadow masks with W/L of ca. 6/1 and 1.5/1. The active semiconductor film areas for these two values of W/L were ca. 4 mm^2 and (3−4) × 10^{-2} mm^2, respectively. The organic semiconductors were deposited at a rate of 2−3 Å/s under a pressure of 2.0×10^{-6} Torr to a final thickness of 500 Å. Substrate temperature during deposition was controlled by heating or cooling the copper block on which the substrate was mounted. The electrical characteristics were obtained at room temperature in air using a 4145B Hewlett-Packard (HP) semiconductor parameter analyzer.

For morphological characterization, the materials were deposited onto carbon-coated electron microscope grids and Si/SiO_2 chips simultaneously with the FET devices. X-ray diffraction studies were performed on the chips in the reflection mode at 40 kV and 25 mA. A 2 kW Rigaku X-ray generator was used as a source of Ni-filtered Cu Kα radiation. The films on the grids, used for electron microscopy, were shadowed with Pt/C at $\tan^{-1}$ 0.5 and lightly carbon-coated in a vacuum evaporator before examination using a JEOL transmission electron microscope operated at 100 kV.

5,5′-Diiodo-2,2′-bithiazole (2). To a solution of diisopropylamine (2.1 mL, 15 mmol) in 10 mL of THF at −78 °C was

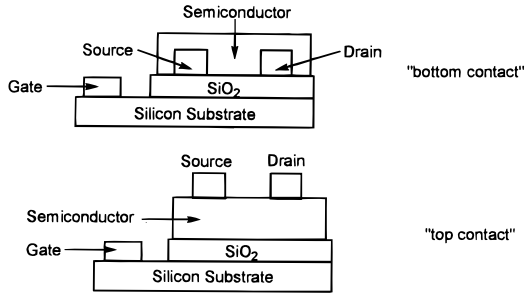

Figure 1. Schematic FET structure showing two different device configurations.

added ^{n}BuLi (4.4 mL, 2.5 M in hexanes, 11 mmol) via syringe. The solution was allowed to warm to room temperature for 5 min and was then recooled to −78 °C. 2,2′-Bithiazole (0.84 g, 5 mmol) in 10 mL of THF was then added. After the mixture was stirred at −78 °C for 1 h and warmed to room temperature for an additional hour, iodine (2.92 g, 11.5 mmol) in 20 mL of THF was added. Stirring was continued for another hour, after which saturated $Na_2S_2O_5$ (50 mL) was added followed by addition of ether and subsequent extraction. The organic layer was separated, dried over $MgSO_4$, and decolorized with active carbon. After the solvent was removed, the resulting brown solid was further recrystallized from a mixture of chloroform and acetonitrile (1:1) to yield 1.4 g of light brown crystal (64%). ^{1}H NMR ($CDCl_3$) δ 7.87 (s, 2H).

5,5′-Bis(5-hexyl-2-thienyl)-2,2′-bithiazole (BHT2Z2). A solution of 2-bromo-5-hexylthiophene (1.48 g, 6 mmol), 5,5′-bis(trimethylstannyl)-2,2′-bithiazole (0.99 g, 2 mmol), and $Pd(PPh_3)_4$ (116 mg, 0.1 mmol) in 25 mL of anhydrous benzene was heated to reflux for 14 h. The solvent was removed and a mixture of ether and hexane (1:1) was added to the residual material. The resulting organic solid was filtered and washed with the mixture of ether and hexane. The solid was then dissolved in hot chloroform, the solution was filtered and concentrated, and the residual solid was sublimed in vacuo to give 0.25 g of bright yellow solid (25%): ^{1}H NMR ($CDCl_3$) δ 7.83 (s, 2H), 7.09 (d, 3.6 Hz, 2H), 6.74 (d, 3.6 Hz, 2H), 2.82 (t, 4H), 1.70 (m, 4H), 1.33 (m, 12H), 0.91 (t, 6H). Anal. Calcd for $C_{26}H_{32}N_2S_4$: C, 62.36; H, 6.44; N, 5.59; S, 25.61. Found: C, 62.11; H, 6.44; N, 5.50; S, 25.33.

5,5′-Bis(5′-hexyl-2-bithienyl)-2,2′-bithiazole (BHT4Z2). A solution of 5-hexyl-5′-tributylstannyl-2,2′-bithiophene (3.37 g, 6.25 mmol), 5,5′-dibromo-2,2′-bithiazole (1.05 g, 2.5 mmol), and $Pd(PPh_3)_4$ (145 mg, 0.13 mmol) in 35 mL of anhydrous toluene was heated to just below reflux for 3 days. The red precipitate was collected from the hot solution and washed with diluted HCl, water, and acetone successively. Recrystallization of the crude product from 50 mL of mesitylene with hot filtering gave 0.49 g of solid. The product was further purified by sublimation to yield 0.37 g of red solid (22%). Anal. Calcd for $C_{34}H_{36}N_2S_6$: C, 61.40; H, 5.46; N, 4.21; S, 28.92. Found: C, 61.13; H, 5.33; N, 4.24; S, 28.81.

5,5′-Bis(5′-hexyl-2-bithienyl)-4,4′-dihexyl-2,2′-bithiazole (BHT4DHZ2). BHT4DHZ2 was obtained from 5-hexyl-5′-tributylstannyl-2,2′-bithiophene and 5,5′-dibromo-4,4′-dihexyl-2,2′-bithiazole following a procedure similar to that described for BHT4Z2. After the reaction, methanol was added. The red precipitate was collected by filtration and washed with methanol. The product was then purified by chromatography [silica gel, hexane/chloroform (2/1)] to give 0.62 g of red solid (74%). Material for analysis and FET fabrication was further purified by sublimation: ^{1}H NMR ($CDCl_3$) δ 7.08 (d, 3.9 Hz, 2H), 7.06 (d, 3.9 Hz, 2H), 7.02 (d, 3.4 Hz, 2H), 6.71 (d, 3.4 Hz, 2H), 2.96 (t, 4H), 2.81 (t, 4H), 1.80 (m, 4H), 1.69 (m, 4H), 1.34 (m, 24 H), 0.90(t, 12H). Anal. Calcd for $C_{40}H_{60}N_2S_6$: C, 66.30; H, 7.26; N, 3.36; S, 23.08. Found: C, 66.32; H, 7.32; N, 3.30; S, 22.83.

Dihexylquinquethiophene (DHα5T). DHα5T was obtained from 5-hexyl-5′-tributylstannyl-2,2′-bithiophene and 2,5-dibromothiophene following a procedure similar to that described for BHT4Z2. Recrystallization of the crude product from mesitylene with hot filtering gave DHα5T as a red solid.

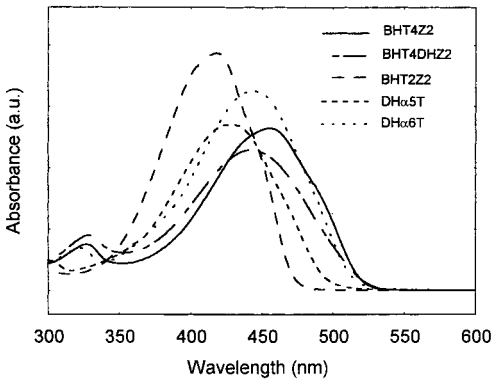

Figure 2. Absorption spectra of the thiazole-containing oligomers and DHα5T in toluene. The spectrum of DHα6T is also given for comparison.

The product was further purified by sublimation at a pressure of ca. 10^{-4} Torr (61%). Anal. Calcd for $C_{32}H_{36}S_5$: C, 66.14; H, 6.25; S, 27.61. Found: C, 66.19; H, 6.24; S, 27.59.

Results and Discussion

All of the compounds were synthesized using different variations of the Stille coupling reaction that has been widely used for the synthesis of oligothiophenes.[13,21,22] However, the yields of the thiazole-containing oligomers were considerably lower than those of the oligothiophenes, except for compound BHT4DHZ2. Various side products generated from the dimerization of the diiodo- or bis(trimethylstannyl)bithiazole, as well as the coupling reaction of the dimers with the corresponding bis(tributylstannyl)bithiophene or dibromothiophene, were detected. Substituting the 4- and 4′-positions of the bithiazole molecule with hexyl chains noticeably subdued the dimerization, possibly due to the increased steric hindrance, and therefore increased the Stille coupling yield. Furthermore, the addition of the two hexyl substituents on the bithiazole moiety greatly improved the solubility of the resulting oligomer. As a result, BHT4DHZ2 is very soluble in most common organic solvents and could be purified by simple chromatography. All of the other compounds are soluble in aromatic solvents such as toluene, mesitylene, chlorobenzene, and trichlorobenzene. As a comparison, both BHT4Z2 and DHα5T have better solubility in organic solvents than the corresponding DHα6T, making them good candidates for liquid-phase device fabrication.

The compounds were characterized both spectroscopically and analytically. The elemental analysis results were consistent with all of the proposed structures. The UV/vis absorption spectra of these compounds in toluene are shown in Figure 2. As expected, the absorption maxima of these compounds increase with the conjugation length. For example, compound BHT4Z2 has an absorption maximum at 455 nm, which is 38 nm red-shifted compared to compound BHT2Z2. On the other hand, compound BHT4DHZ2 has an absorption maximum which is 14 nm blue-shifted relative to compound BHT4Z2, possibly due to the reduced coplanarity caused by the steric hindrance between the hexyl-substituted

(21) Wei, Y.; Yang, Y.; Yeh, J.-M. *Chem. Mater.* **1996**, *8*, 2659.
(22) Wu, R.; Schumm, J. S.; Pearson, D. L.; Tour, J. M. *J. Org. Chem.* **1996**, *61*, 6906.

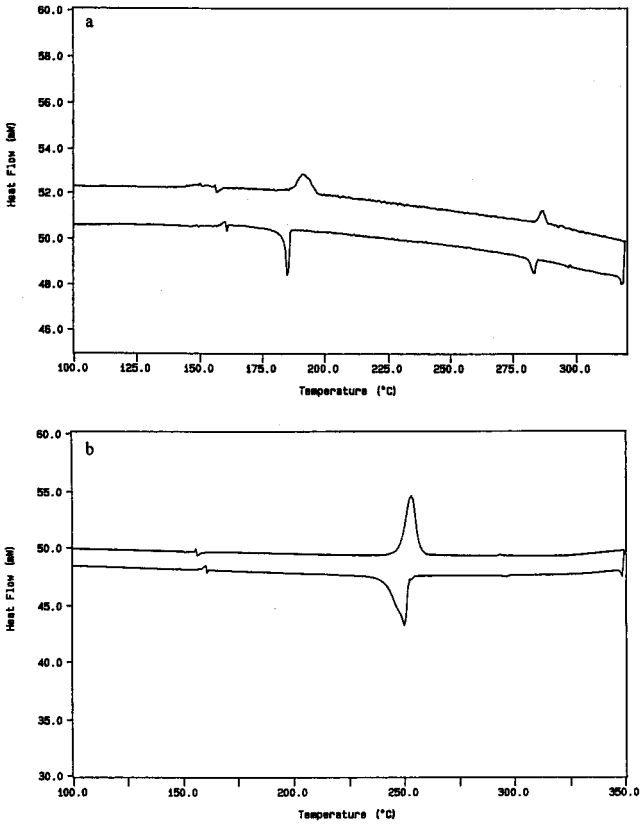

Figure 3. DSC thermographs of (a) BHT4Z2 and (b) DHa5T under a N_2 atmosphere.

Table 1. Properties of Thin Films on Si/SiO_2 Evaporated at Room Temperature

compound	T_m (°C)[a]	T_c(°C)[b]	repeat spacing (Å)	mobility (cm^2/V s)
BHT4Z2	191	285	28	0.0077
BHT4DHZ2	83	92	24	0.00035
BHT2Z2	111	185	18, 14	0.00002[c]
T2Z2	222[d]		56, 12	0.00001[c]
DHα5T	254[d]		30	0.026

[a] Crystal-to-liquid crystal transition temperature. [b] Liquid crystal-to-isotropic transistion temperature. [c] Bottom contact. [d] Melting point.

thiazole and the adjacent thiophene ring. Compared to DHα6T, BHT4Z2 also has a 12 nm red-shift in absorption maxima.

The thermal properties of these compounds were determined by a heating−cooling cycle using DSC under nitrogen. All of the compounds exhibit at least one transition temperature, as illustrated in Figure 3. The general trend is that the transition temperature decrease as the number of thiophene and thiazole rings decreases, as in the case of BHT4Z2 and BHT2Z2 (Table 1). The addition of alkyl substituents onto the rings also decreases the transition temperatures dramatically, i.e., BHT2Z2 vs T2Z2, BHT4DHZ2 vs BHT4Z2. Compound BHT4Z2 has a crystal-to-liquid crystal (LC) transition at 191 °C and a LC-to-isotropic transition at 285 °C, both of which are lower than the melting point of the corresponding DHα6T (>300 °C). The thiazole compounds also have lower melting points than their all-thiophene analogues.

The transistor behavior of these compounds was studied using the device structures shown in Figure 1.

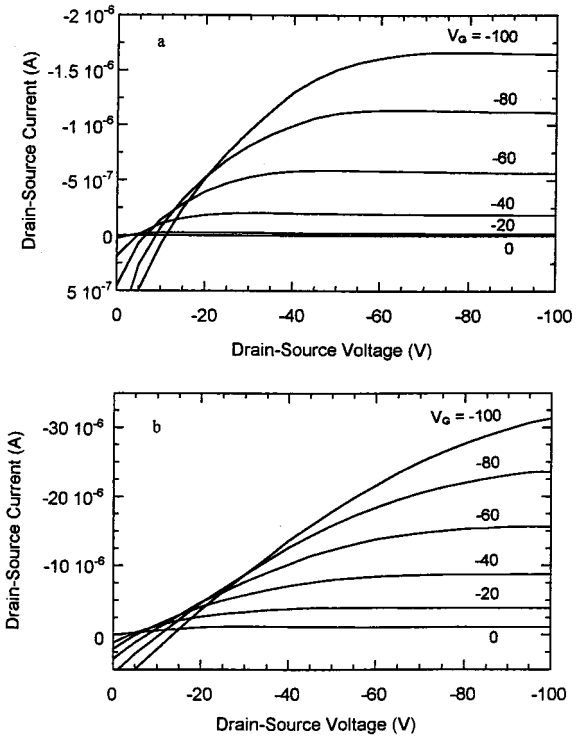

Figure 4. Electrical characteristics of (a) BHT4Z2 deposited at 30 °C ("top contact", $W/L = 6$) and (b) DHα5T deposited at 155 °C ("top contact", $W/L = 1.5$). The increasing deviations from zero current at zero drain-source voltage with increased gate voltage are caused by leakage through the dielectric.

Table 2. Field-Effect Mobilities for Samples of BHT4Z2 and DHα5T Evaporated at Different Substrate Temperatures (T_D)

T_D (°C)	BHT4Z2[a]	DHα5T[a]
30	0.0077	0.026[b]
55	0.011	0.032
80	0.0067	0.034
105	0.0031	0.037
155		0.08−0.1
175		0.064
180	0.0023	
200		0.024

[a] Top contact. [b] At this temperature, devices fabricated using bottom contact geometry generally have mobilities of 0.05−0.07.

All of the compounds operated as typical p-channel transistors in the accumulation mode. Figure 4a shows the current−voltage curves of a BHT4Z2-based FET device (T_D = 30 °C) at different gate voltages. The field-effect mobilities were estimated in the saturation regime using eq 1

$$I_{ds} = (W/2L)mC_i(V_g - V_0)^2 \quad (1)$$

where I_{ds} is the drain-source current in the saturated region, W and L are the channel width and length, respectively, m is the field-effect mobility, C_i is the capacitance per unit area of the insulating layer, and V_g and V_0 are the gate voltage and the threshold voltage. The field-effect mobilities of all films evaporated at room temperature are summarized in Table 1. Mobilities obtained on films of BHT4Z2 and DHα5T at different deposition temperatures are listed in Table 2. Among the thiazole-containing oligomers, the highest mobility was achieved with BHT4Z2 (ca. 0.0077 cm^2/V s at 30

°C). The mobilities of other thiazole oligomers are at least 1 order of magnitude lower than that of BHT4Z2. It is interesting that BHT4DHZ2 has a finite mobility and an edge-on orientation (see below) despite the internal alkyl substituents.

The mobility is strongly dependent on the deposition temperature T_D. For BHT4Z2, the field-effect mobility increases with T_D to a maximum of ca. 0.011 cm^2/V s and then decreases as the temperature is further increased. The fact that BHT4Z2 devices have lower mobilities than corresponding DHα6T devices could be partially due to less efficient charge injection, caused by the decreased electron-donating ability of the BHT4Z2 molecule, and a possibly greater mismatch between the work function of the electrodes and the accessible hole energy levels of the film. On the other hand, the off currents of the BHT4Z2 devices are much lower than those of the DHα6T devices. On/off current ratios of greater than 10^4 without depletion can be routinely obtained from devices operating in air, eliminating the need of strict oxygen exclusion.

To further test the chemical stability of the BHT4Z2 devices, the threshold voltage is estimated as a function of air exposure. It is expected that doping of a p-type transistor will result in a positive threshold voltage and exposure to oxygen will shift the threshold voltage to a larger positive value. The threshold voltage of BHT4Z2 devices evaporated at 30 °C is calculated to be −11 V. Exposure of the devices to air for 35 days causes little change in the threshold voltage value, indicating no detectable p-doping by oxygen. As a comparison, the threshold voltage of DHα6T devices is also measured under the same experimental conditions. The freshly evaporated film has a threshold voltage of −3 V. After the film is exposed to air for 5 days, the threshold voltage is dramatically shifted to (*positive*) 15 V. Continuing exposure of the film to air for 30 days further shifts the threshold voltage to (*positive*) 32 V. We note that similar results were also obtained on DHα6T by Horowitz et al. recently.[23]

As shown in Figure 4b, a distinct field effect was also observed with DHα5T devices. As with other dihexyl-substituted oligothiophenes and BHT4Z2, the field-effect mobilities of DHα5T also increase with deposition temperature to a maximum value and then decrease as substrate temperature further increases. The highest mobility (∼0.1 cm^2/V s) was obtained at 155 °C for top-contact FETs, which is almost 2 orders of magnitude higher than the highest reported mobility of all substituted and unsubstituted α5T compounds.[15,24,25] It is worth noting that this value is also close to the mobility observed in single-crystal films of DHα4T and slightly higher than that of DHα6T.

The morphology and solid-state structure of the sublimed films were studied using bright-field transmission electron microscopy, X-ray diffraction, and electron diffraction techniques. Transmission electron microscopy of films of BHT4Z2 and DHα5T on carbon-coated grids reveals flat and thin crystals parallel to the substrate (Figures 5a−e), as in the cases of DHα4T and DHα6T. The crystals of DHα5T exhibit very typical crystallographic features such as screw dislocations and terraces (Figure 5d,e). The grain sizes of the crystals of both compounds increase with deposition temperature. As the temperature further increases, however, gaps between crystals also become visible, which cause discontinuities at the grain boundaries (Figure 5c,e). Similar to DHα4T and DHα6T, there are optimal deposition temperatures for BHT4Z2 and DHα5T. Films deposited at these temperatures seem to present the best compromise between large grain sizes and space-filling grain connectivity, and therefore give the highest mobilities.

Electron micrographs of compounds T2Z2 and BHT2Z2 reveal totally different morphologies. As shown in Figure 5f, instead of flat lamellae, T2Z2 shows separated, three-dimensional, micron-sized crystals oriented at different directions, a less favorable morphology for EFTs. A similar morphology was also obtained in BHT2Z2 films. These less ordered, discontinuous morphologies are almost certainly responsible for the low mobilities observed in these compounds.

We tested one additional compound as an aza-substituted analogue of the known hole-transporting polyacenes: TAN. This compound was synthesized according to the two-step literature procedure via dehydrative condensation of 2,3-dihydroxy-1,2,3,4-tetrahydroquinoxaline and 1,2-phenylenediamine in polyphosphoric acid, followed by lead tetraacetate oxidation of the dihydro condensation product.[26] Sublimation of TAN at several temperatures on a variety of substrates always resulted in extremely discontinuous films, in many cases consisting of three-dimensional crystallites separated by spaces as large as the faces of the crystallites. This is in marked contrast to pentacene, which not only forms two-dimensional, continuous films but even forms single crystalline films under some conditions. The surface of a single crystal pentacene film, used as a potentially epitaxial template, was not sufficient to overcome the tendency of TAN to solidify from the vapor phase as isolated microcrystals.

From these observations, we may deduce that the quadrupole imparted on an otherwise electrically homogeneous molecule by the imino nitrogens greatly influences the kinetics and/or thermodynamics of the growth of solid films, either by slowing growth in the lateral directions so that vertical growth becomes competitive or by imposing a lateral repulsion that decreases the lateral interactions among the p-systems and destabilizes the crystals. The thermodynamic explanation is consistent with the lower melting points of the thiazole-containing compounds synthesized for this study compared to their all-thiophene analogues. The lower mobility of the seemingly well-ordered BHT4Z2 compared to DHa6T may also be due to decreased intermolecular π-interaction.

X-ray diffraction of the films grown on Si/SiO_2 shows sharp peaks corresponding to the molecular repeat spacings (Table 1). Films of BHT4Z2 and BHT4DHZ2 adopt an edge-on orientation. The repeat spacing of

(23) Horowitz, G.; Hajlaoui, R.; Bouchriha, H.; Bourguiga, R.; Hajlaoui, M. *Adv. Mater.* **1998**, *10*, 923.

(24) Hajlaoui, R.; Horowitz, G.; Garnier, F.; Arce-Brouchet, A.; Laigre, L.; Kassmi, A. E.; Demanze, F.; Kouki, F. *Adv. Mater.* **1997**, *9*, 389.

(25) Waragai, K.; Akimichi, H.; Hotta, S.; Kano, H.; Sakaki, H.; *Synth. Met.* **1993**, *55−57*, 4053.

(26) Badger, G. M.; Nelson, P. J. *Austral. J. Chem.* **1963**, *16*, 445.

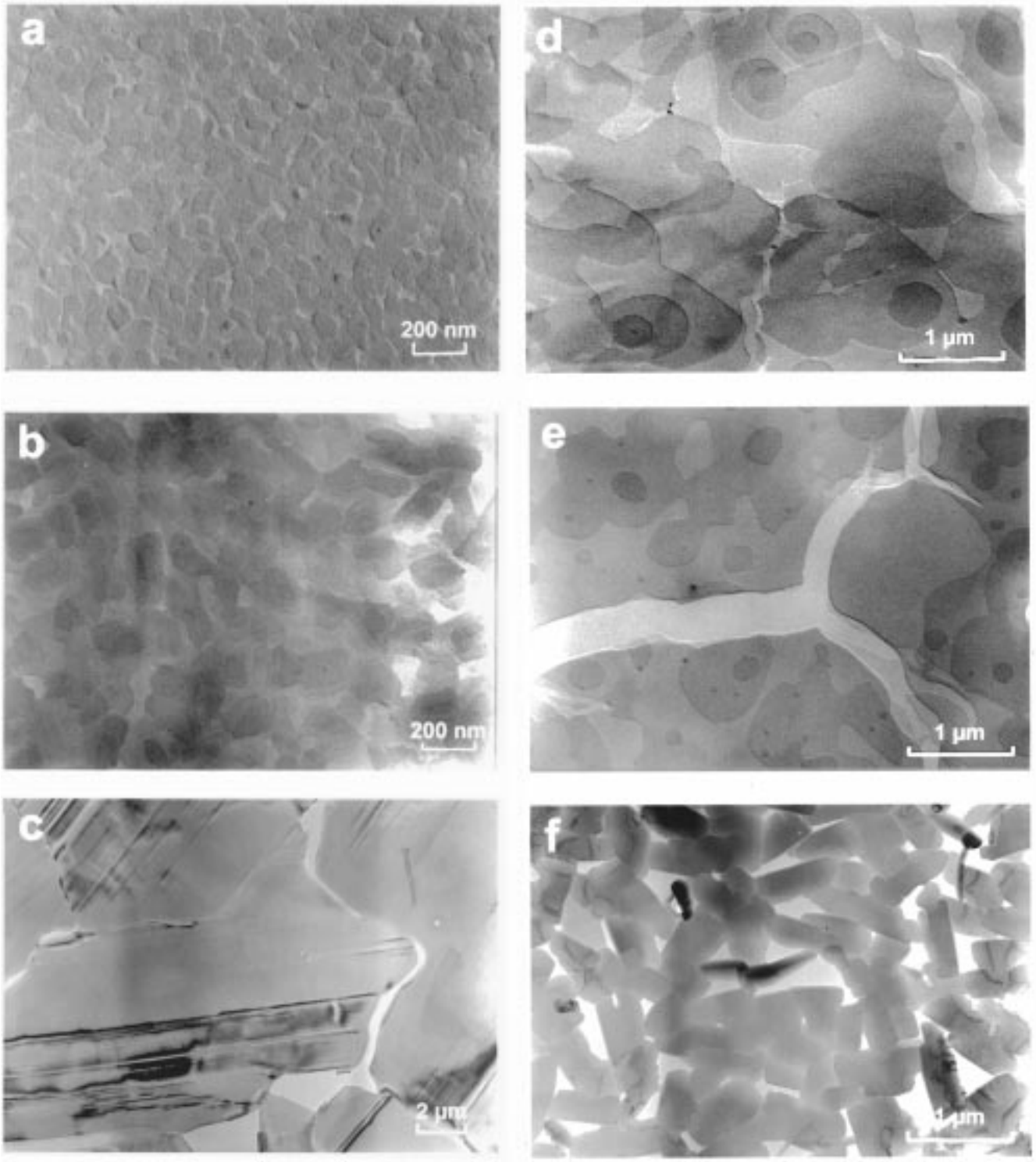

Figure 5. Transmission electron micrographs obtained for BHT4Z2, DHα5T, and T2Z2 at different deposition temperatures (T_D): (a) BHT4Z2 (T_D = 30 °C), (b) BHT4Z2 (T_D = 55 °C), (c) BHT4Z2 (T_D = 180 °C), (d) DHa5T (T_D = 155 °C), (e) DHa5T (T_D = 175 °C), (f) T2Z2 (T_D = 30 °C).

BHT4Z2 is consistent with the schematic representation depicted in Figure 6 in which the two hexyl chains are projected nearly perpendicular to the substrate and the conjugated cores are bent at an angle. This orientation is essentially the same as what has been reported for α,ω-dialkylsexithiophenes.[13,14] Compound BHT4DHZ2 probably has this orientation but with some interdigitation. For compounds T2Z2 and BHT2Z2, two unrelated sets of diffraction peaks were observed, suggesting either two different polymorphs or two different orientations of crystals.

Films of DHα5T evaporated at high temperatures were also examined using electron diffraction. Very surprisingly, despite the large size, regularity, and crystallographic features of the DHα5T films, only weak, poor, and indistinct diffraction spots (Figure 7a) were observed under normal observation conditions, i.e., with the electron beam perpendicular to the lamellae and to the film. However, at a tilt angle of ~30° about an axis normal to the *b* crystallographic direction, a very intense

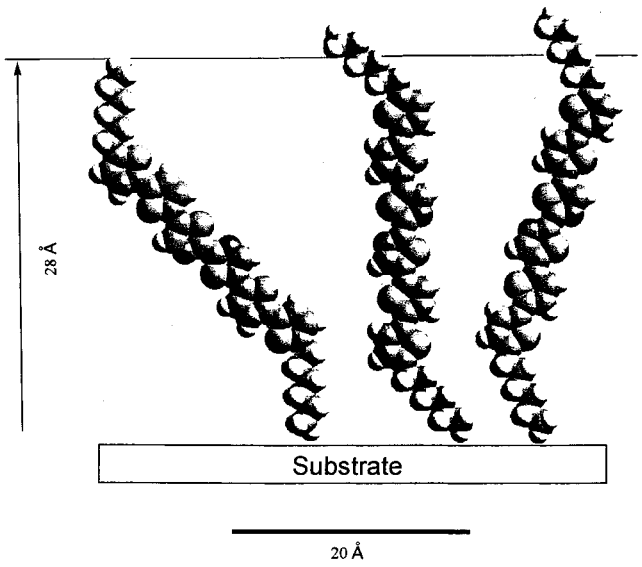

Figure 6. Molecular models of BHT4Z2 hypothetical substrate arrangements.

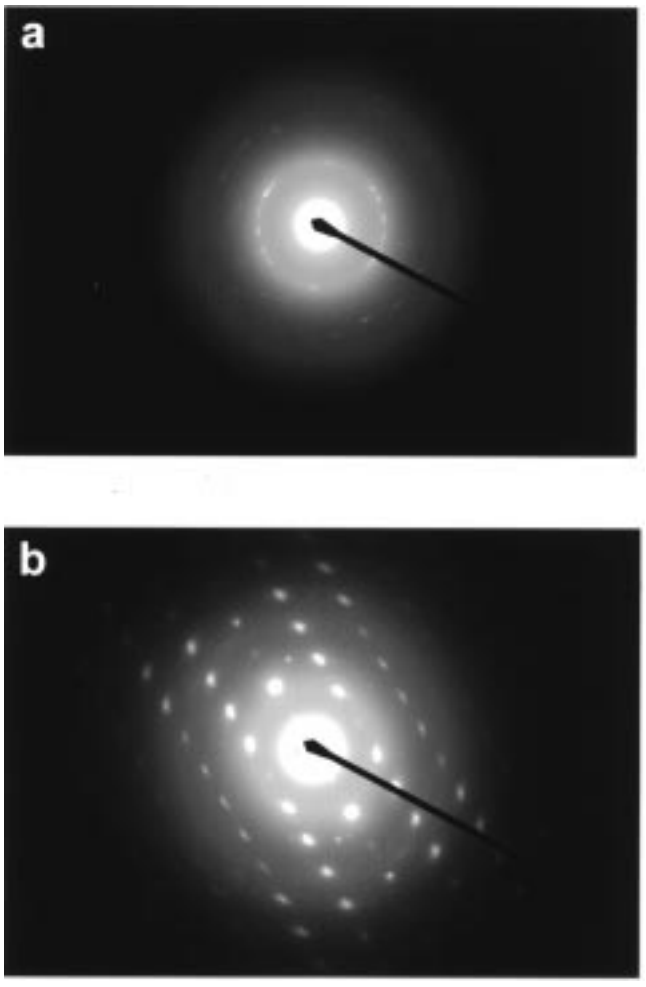

Figure 7. Selected-area electron diffraction patterns of DHα5T film deposited at $T_D = 175$ °C with the electron beam (a) perpendicular to the substrate and (b) at a tilt angle of ~30° about an axis normal to the *b* crystallographic direction.

and rich diffraction pattern was obtained (Figure 7b). This sharp, spotty pattern arises from essentially single crystalline areas covering tens of microns in diameter, similar to what we found for DHα4T samples.[14] As in the case of DHα4T, we believe that the high mobilities obtained in DHα5T at high deposition temperatures are correlated with the single-crystal nature of the films. At a deposition temperature of 175 °C, the diffraction pattern (after tilting) reveals a rectangular lattice with axes of 5.46 and 7.72 Å. The lattice symmetry, systematic absences, *d* spacings, and reflection intensities are very similar to those in the even-numbered oligothiophenes (α4T, α6T, and α8T) studied earlier.[14,27−29] The orientation of the DHα5T molecules on the substrate, however, differs in that they are inclined to the substrate at ~30°, as suggested by the electron diffraction patterns together with X-ray diffraction data. Tilting is specifically about an axis that is approximately normal to the molecular axis and normal to the *b*-axis of the unit cell (in the Garnier α6T unit cell,[27] this tilt axis would correspond to the $(40\bar{1})$ plane normal). We note that a perpendicular orientation has been reported for α5T by Hailaoui et al.[24] Reasons for the molecular inclinations in DHα5T are not known, but it does not appear to be associated with the reduced length of the molecule, since DHα4T, which is even shorter, orients on the substrate in the same way as α6T and α8T.

Conclusion

The synthesis, thin-film morphology, and hole mobility in FETs based on several oligothiophene analogues with reduced electron-donating ability have been explored. The incorporation of thiazole rings into oligothiophenes was found to have profound effects on the properties of the evaporated films. The thiazole-containing compounds generally have lower melting points and better solubility than the corresponding oligothiophenes. FET devices fabricated from the thiazole-containing compounds also showed improved chemical stability due to the reduced susceptibility to p-doping. However, the tradeoff is their lower field-effect mobility, which is possibly caused by the larger charge injection barrier and poorer ordering in the films. DHα5T films exhibit high field-effect mobility, which is probably a consequence of the single-crystal-like morphology of the films. At the higher deposition temperatures, a projected rectangular lattice having axes of 5.46 and 7.72 Å could be clearly identified. The orientation has the molecules tilted at a specific angle of ~30° relative to the substrate. Both compounds BHT4Z2 and DHα5T have better solubility than DHα6T, making them attractive candidates for the fabrication of liquid-phase-processed FET devices.

Acknowledgment. We would like to thank our colleagues Zhenan Bao, Karl R. Amundson, Yen-Yi Lin, and Ananth Dodabalapur for useful discussions.

CM980672C

(27) Lovinger, A. J.; Davis, D. D.; Dodabalapur, A.; Katz, H. E.; Torsi, L. *Macromolecules* **1996**, *29*, 4952.
(28) Horowitz, G.; Bachet, B.; Yassar, A.; Lang, P.; Demanze, F.; Fave, J.-L.; Garnier, F. *Chem. Mater.* **1995**, *7*, 1337.
(29) Hailaoui, R.; Fichou, D.; Horowitz, G.; Nessakh, B.; Constant, M.; Garnier, F. *Adv. Mater.* **1997**, *9*, 557.